

INFLUENCE OF MICRO ASPERITY-VALLEY ON THE SURFACE OF FORGING TOOLS ON TRIBOLOGICAL CONDITIONS

HIROYUKI SAIKI¹, YASUO MARUMO^{1,A}, LIQUN RUAN¹, JUNPEI KOZASA¹

¹Department of Mechanical System Engineering, Graduate School of Science and Technology, Kumamoto University, 2-39-1 Kurokami, Kumamoto 860-8555, Japan

^amarumo@gpo.kumamoto-u.ac.jp

Abstract

The relationship between apparent coefficient of friction, surface roughness and the yield stress of solid lubricant is examined using rigid-plastic finite element analysis. The minimum lubricant thickness decreases significantly when $\sigma_{YL}/p < 1/10$, where σ_{YL}/p is the yield stress of solid lubricant and p is the tool contact pressure. When the friction shear factor is low, the apparent coefficient of friction is strongly influenced by the slope angle. The apparent coefficient of friction decreases with the decrease in the yield stress of the solid lubricant. Although the apparent coefficient of friction increases with increasing the friction shear factor of the tool-solid lubricant interface, the apparent coefficient of friction remains sufficiently small in the case that the yield stress of the solid lubricant is approximate one tenth of that of the workpiece material. Tribological conditions should be optimized so that the shear friction resistance of solid lubricant should be sufficiently small and the lubricant film should not break.

Key words: forging, geometry of surface roughness, tribological conditions, solid lubricant, lubricant film thickness

1. INTRODUCTION

For tools of cold die forging, the surface of the tool where a large slide is caused is finished up very smoothly by lapping operation. This decreases the interfacial friction, and prevents seizure and the breakage of lubricant films. Consequently, the quality of finished products is improved. On the other hand, there is also a try to entrap lubricants by setting micro asperity-valley area on the tool surface to maintain the lubricated condition. Even if the surface has been finished like a mirror surface, there is surface roughness of approximately 0.01-10 μm on the metal surface. The geometry of the micro grooves and asperities in the surface roughness can strongly influence the tribological conditions including contact state and lubricant behavior in the tool-workpiece interface. Interactions between solid lubricant, workpiece material and surface roughness

(micro grooves and asperities) should be revealed. Various studies have been conducted on tribological conditions in the contact interface (Bowden & Tabor, 1964; Wanheim & Bay, 1978; Challen & Oxley, 1979; Wilson, 1990; Geiger et al., 1992; Stancu-Niederkom et al., 1994; Sheu et al., 1998; Steinhoff et al., 1999; Ruan et al., 2005; Saiki et al., 1996; Saiki et al., 2001; Altan et al, 1982; Im, 1984). In our previous report, the characteristics of contact pressure distribution, initial filling mode to the unevenness of roughness and surface expansion were investigated.

This study aims at investigating how roughness on the tool surface influences tribological conditions using rigid-plastic finite element analysis. The relationship between apparent coefficient of friction, surface roughness and the yield stress of solid lubricant was examined.

2. FUNDAMENTAL FEATURES OF VARIATION IN THE FILM THICKNESS OF SOLID LUBRICANTS

In order to investigate fundamental features of the variation in the film thickness of solid lubricant, the analysis that a cylindrical punch is pressed in a S15C workpiece with 20 μm thick lubricant was conducted. In the analysis, a rigid plastic FEM code which was developed by the authors was used. As shown in figure 1, the punch has the contact angle α and the flat region of 2 mm diameter at the punch bottom. The initial lubricant thickness was assumed to be $\delta_0 = 20 \mu\text{m}$ and the yield stress of solid lubricant was varied. Figure 2 shows an example of the state of lubricant and the contact pressure distribution between the punch and the lubricant for $\alpha = 3^\circ$. It is seen that the lubricant thickness decreases near the periphery of the punch flat region and the maximum contact pressure occurs there. The contact pressure, p , ranges from 600 MPa to 900 MPa near the location where the lubricant thickness becomes the thinnest. Results of numerical simulation on lubricant thickness are shown in figures 3 and 4. Figure 3 shows the influence of the yield stress of the solid lubricant on the minimum lubricant thickness for $\alpha = 3^\circ$. It is seen that the minimum lubricant thickness decreases significantly when the yield stress of the solid lubricant decreases below 100 MPa, i.e., $\sigma_{YL}/p < 1/10$.

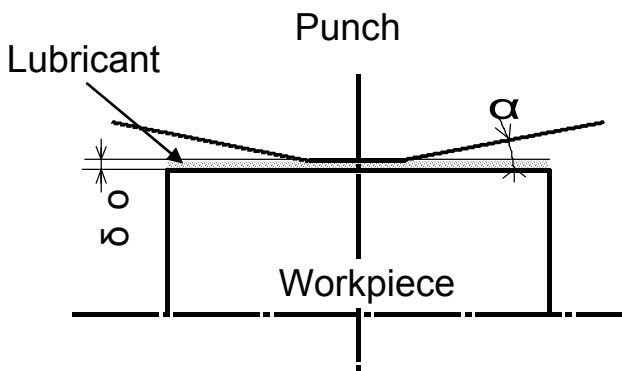


Fig. 1. Analysis model for calculating solid lubricant thickness without the consideration of surface roughness.

Figure 4 shows the influence of contact angle on the minimum lubricant thickness for $\sigma_{YL} = 50 \text{ MPa}$. The minimum lubricant thickness decreases with increasing the contact angle. When the contact angle is 10° , the minimum lubricant thickness decreases to 9 μm . Tribological conditions should be optimized so that the shear stress should be small and the lubricant film should not break.

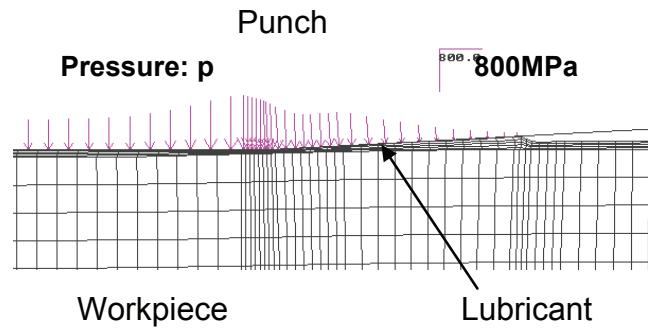


Fig. 2. An example of simulation result (contact pressure and state of solid lubricant).

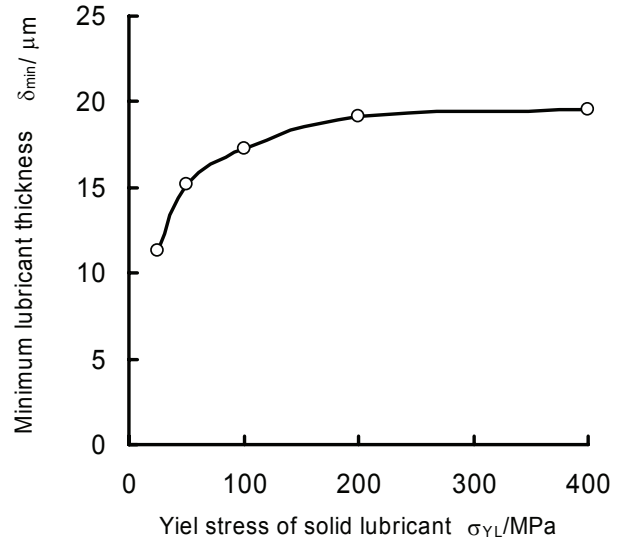


Fig. 3. Relationships between minimum lubricant thickness and yield stress of solid lubricant.

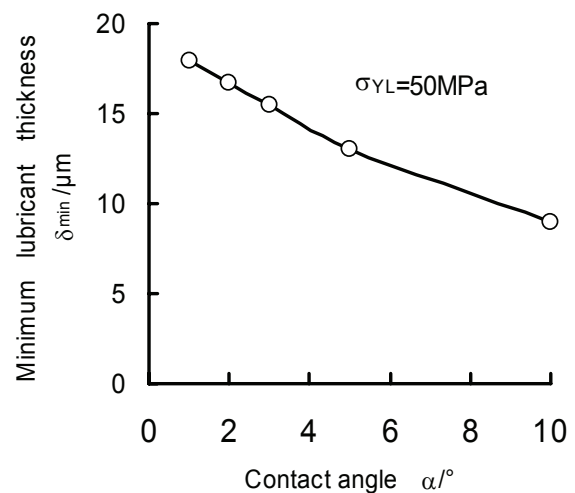


Fig. 4. Relationships between minimum lubricant thickness and contact angle.

3. SURFACE STRUCTURE AND TRIBOLOGICAL CHARACTERISTICS

In this section, the relationship between the geometry of surface roughness and the coefficient of friction on the region with surface roughness while



the workpiece material flows was examined using rigid-plastic finite analysis. Figure 5 shows the axis-symmetric deformation model used in this study. The die 1 is moved at the velocity V_s in the radial direction. The die 2 is moved at the velocity V_s in the radial direction and at the velocity V_i in the axial direction. The die 3 is moved at V_i in the axial direction. The surface roughness region is applied partially at the right of the bottom face of the upper stationary punch. Friction on the tool surface is ignored excluding the surface roughness region. The flow curves of material A and B is expressed by $\sigma_y = 800(0.001 + \epsilon)^n$ [MPa]. The surface roughness has a wavy shape with the height h , the tip angle ψ , the slope angle θ and the tip radius r as shown in figure 5.

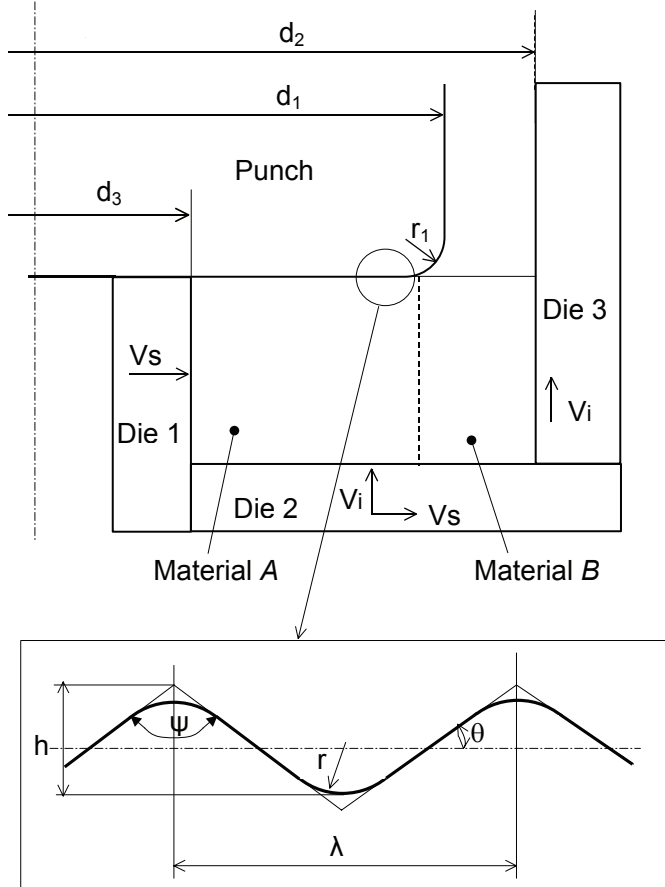


Fig. 5. Analysis model considering surface roughness ($V_s/V_i=1$, A, B: $\sigma_y=800(0.001+\epsilon)^n$).

Friction shear stress τ_f on the surface roughness is given with mk where m is the friction shear factor and k is the shear yield stress of the workpiece material. The apparent coefficient of friction on the roughness region is defined as $\mu_a = Fr/Fz$, where Fr is the integration value of the radial component of the contact pressure and Fz is that of the axial component of the contact pressure. μ_a on the flat surface region without roughness is mk/p_m . Here, p_m is the

average contact pressure on the flat region and k is the shear yield stress.

3.1. Influence of slope angle of asperities of roughness region

The influence of the geometry of roughness ($\theta = \pi - \psi$) and the friction shear factor on the apparent coefficient of friction was estimated by numerical simulation as shown in Figure 6. The n -value of the workpiece and V_s/V_i are assumed to be 0.1 and 1, respectively. The tip radius was $1.2h$ when $\theta = 20^\circ$ and 30° , and $10h$ when $\theta = 5^\circ$ and 10° . Apparent coefficient of friction under the friction shear factor $m = 0$ is also calculated as $\mu_a = Fr/Fz$ when the workpiece material gets over the asperity of the surface roughness. μ_a increases linearly with increasing the slope angle θ and approaches the maximum value of 0.2-0.25. The average contact pressure on the punch surface without roughness is $4k - 5k$ for this extrusion condition.

The apparent coefficient of friction μ_a increases as the friction shear factor m in the region with roughness increases. When m is low, μ_a is strongly influenced by θ . In addition to the above-mentioned parameter, apparent coefficient of friction is somewhat influenced by the tip corner radius and the work-hardening exponent n of the workpiece material. For examples, μ_a increases from 0.112 to 0.123 almost proportionally under $\theta = 15^\circ$ and $m = 0$ as the work-hardening exponent n increases from 0 to 0.2. This variation trend in μ_a approximately corresponds to actual variation trend in μ_a .

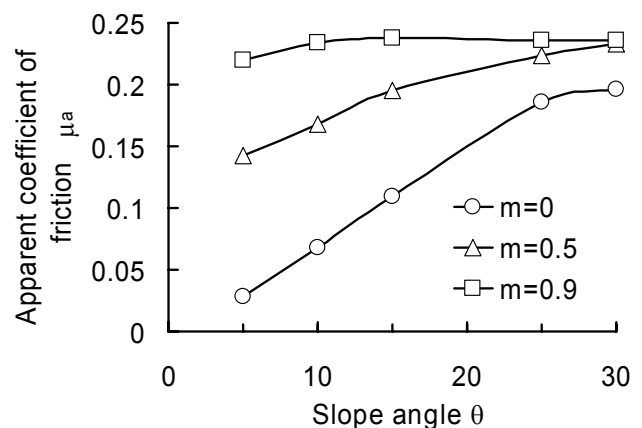


Fig. 6. Relationships between apparent coefficient of friction μ_a and slope angle θ .

3.2. Effect of the yield stress of solid lubricant

Behavior of the lubricant film with the yield stress σ_{YL} and the average film thickness $2.5h$ ($h =$



R_{max}) was analyzed. We assumed that the solid lubricant film adhered to the workpiece surface and was in contact with the punch at the friction shear factor m_L . Results of numerical simulation are shown in figures 7 and 8. Figure 7 shows the influence of the yield stress of the solid lubricant. The apparent coefficient of friction μ_a decreases with the decrease in the yield stress of the solid lubricant. The apparent coefficient of friction becomes sufficiently small when the yield stress of the lubricant is approximate one tenth or less of that of the workpiece material. Figure 8 shows the influence of the friction shear factor m_L on the apparent coefficient of friction under $\sigma_{YL} = 50$ MPa. μ_a increases with increasing m_L . However, μ_a remains sufficiently small in the case of $\sigma_{YL} = 50$ MPa, i.e., in the case that the yield stress of the solid lubricant is approximate one tenth that of the workpiece material.

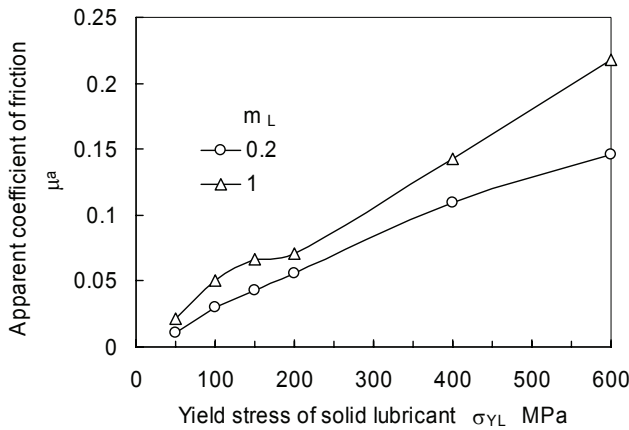


Fig. 7. Relationships between apparent coefficient of friction μ_a and yield stress of solid lubricant σ_{YL} .

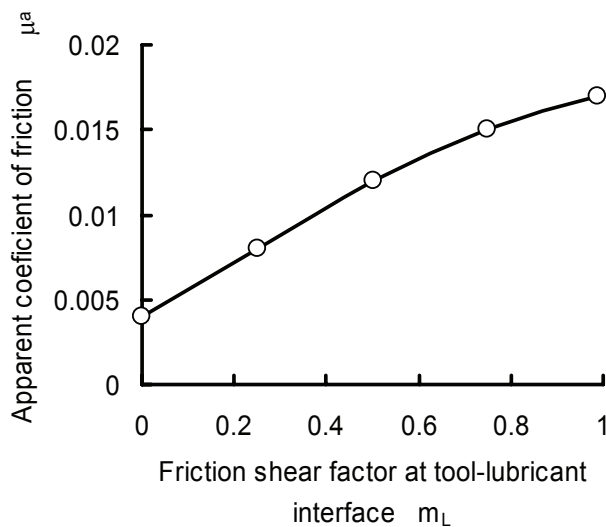


Fig. 8. Relationships between apparent coefficient of friction μ_a and friction shear factor at tool-lubricant interface m_L .

The results of numerical simulation obtained in this study can explain variation trend in μ_a which was observed in actual manufacturing sites, and become a guideline for selecting solid lubricants. Hereafter, we will improve the analysis model and the estimation method of solid lubricants based on corresponding experiments which will be conducted.

4. SUMMARY

The relationship between apparent coefficient of friction, surface roughness and the yield stress of a solid lubricant is examined using rigid plastic finite element analysis. The following results were obtained.

- 1) The minimum lubricant thickness decreases significantly when $\sigma_{YL}/p < 1/10$, where σ_{YL} is the yield stress of solid lubricant and p is the tool contact pressure.
- 2) The minimum lubricant thickness decreases with increasing the contact angle.
- 3) The apparent coefficient of friction increases with increasing the slope angle of surface asperities and approaches the maximum coefficient of friction, i.e., 0.25-0.2.
- 4) The apparent coefficient of friction increases as the friction shear factor in the region with roughness increases.
- 5) When the friction shear factor is low, the apparent coefficient of friction is strongly influenced by the slope angle.
- 6) The apparent coefficient of friction decreases with the decrease in the yield stress of the solid lubricant.
- 7) The apparent coefficient of friction increases with increasing the friction shear factor. However, the apparent coefficient of friction remains sufficiently small in the case that the yield stress of the lubricant is approximate one tenth that of the workpiece material.

REFERENCES

Bowden, F. P. and Tabor, D., 1964, *The Friction and Lubrication of Solids*, Oxford University Press.
 Wanheim, T. and Strandell, P.O., 1978, A model for friction in metal forming process, *Ann. of CIRP*, 27, 189-194.
 Challen, J.M. and Oxley, P.L.B., 1979, An explanation of the different regimes of friction and wear using asperity deformation models, *Wear*, 53, 229-243.
 Wilson, W.R.D, 1990, Mixed Lubrication in metal forming processes, *Advanced Technology of Plasticity 1990*, 4, 1667-1676.



- Geiger, M., Engel, U., Vollersten, F., 1992, In situ ultrasonic measurement of the real contact area in bulk metal forming, *Ann. of CIRP*, 41-1, 255-258.
- Stancu-Niederkom, S., Engel, U., Geiger, M., 1994, Ultrasonic investigation of friction mechanism in metal forming, *J. Mat. Proc. Technol.*, 45, 613-618.
- Sheuhoff, S., Hector, L.G., Richmond, O., 1998, Controlled wear as mechanism for the design of geometrically defined nanometric surface structure on forming tools, Tool surface topographies for controlling friction and wear in metal-forming processes, *Trans. ASME, J. Tribology*, 120, 517-527.
- Stein, K., Kapoor, A., Guillon, N., 1999, *Advanced Technology of Plasticity 1999*, 1, 265-270.
- Ruan, L., Saiki, H., Marumo, Y., Imamura, Y., 2005, Evaluation of coating-based lubricants for cold forging using the localized rod-drawing test, *Wear*, 259, 1117-1122.
- Saiki, H., Zhan, Z., Marumo, Y., Ando, H., 1996, Evaluation of thermal contact resistance in hot and warm forging, *Advanced Technology of Plasticity 1996*, 1, 457-460.
- Saiki, H., Marumo, Y., Minami, A., Sono, T., 2001, Effect of the surface structure on the resistance to plastic deformation of a hot forging tool, *J. Mat. Proc. Technol.*, 113, 22-27.
- Altan, T., Semiatin, S.L., Collings, E.W., Wood, V.E., 1982, Determination of the interface heat transfer coefficient for non-isothermal bulk-forming processes, *Trans. ASME, J. Eng. Indst.*, 109, 49-57.
- Im, Y.T., 1984, Investigation of heat transfer and simulation of metal flow in hot upsetting, *Trans. ASME, J. Eng. Indst.*, 111, 337-343.

WPLYW KSZTAŁTU POWIERZCHNI NARZĘDZI NA PARAMETRY TRYBOLOGICZNE.

Streszczenie

Zależności pomiędzy współczynnikiem tarcia, chropowatością powierzchni i granicą plastyczności środka poślizgowego w formie stałej są badane w niniejszej pracy z wykorzystaniem sztywno plastycznego modelu elementów skończonych. W pracy przeprowadzono szczegółową dyskusję zależności pomiędzy wymienionymi czynnikami, określając zoptymalizowane parametry trybologiczne prowadzenia procesu.

Submitted: October 20, 2006

Submitted in a revised form: December 4, 2006

Accepted: December 6, 2006

